



# Thermal Radiation in Nanofluid Penetrable Flow Bounded with Partial Slip Condition

Nadia Diana Mohd Rusdi<sup>1</sup>, Siti Suzilliana Putri Mohamed Isa<sup>1,2,\*</sup>, Norihan Md. Arifin<sup>1,3</sup>, Norfifah Bachok<sup>1,3</sup>

<sup>1</sup> Institute for Mathematical Research (INSPERM), Universiti Putra Malaysia, 43400 UPM Serdang, Selangor Darul Ehsan, Malaysia

<sup>2</sup> Centre of Foundation Studies for Agricultural Science, Universiti Putra Malaysia, 43400 UPM Serdang, Selangor Darul Ehsan, Malaysia

<sup>3</sup> Department of Mathematics, Faculty of Science, Universiti Putra Malaysia, 43400 UPM Serdang, Selangor Darul Ehsan, Malaysia

## ARTICLE INFO

### Article history:

Received 24 June 2021

Received in revised form 27 July 2021

Accepted 28 July 2021

Available online 8 August 2021

### Keywords:

Dual solutions; nanofluid; thermal radiation; boundary layer flow; suction

## ABSTRACT

Thermal radiation enhances heat transfer, and it is used widely in manufacturing and materials processing applications. Thus, steady two-dimensional boundary layer flow over an exponentially porous shrinking sheet of nanofluids was considered in the influence of thermal radiation related to partial slip boundary conditions and suction. This paper aims to study the nanofluid penetrable flow over an exponentially shrinking sheet with thermal radiation and partial slip. The effects of silver (Ag) nanoparticles with two different types of base fluids named water and kerosene oil are investigated in this study. First, the governing equations and boundary conditions are transformed to a non-linear ordinary differential equation and then solved using *bvp4c* solver. Using Matlab software, it is found that the dual solution exists in some values from the suction parameter. Furthermore, we identified both nanoparticle volume fraction and suction parameter increase, leading to the rise in velocity profile. Moreover, the suction parameter increases both skin friction coefficient and Nusselt number increase.

## 1. Introduction

The significant engineering applications regarding the heat transfer in fluid flow can be observed, such as thermal management of electronic systems, solar collectors, and designing building [1]. Sakiadis [2] was the first to study the fluid flow case over a linearly stretching sheet. Subsequently, the viscoelastic fluid flow over a linear [3] and non-linear [4] stretching sheet are reported. The nanofluid flow beyond a linearly stretching sheet is investigated by Khan *et al.*, [5]. Finally, Mahapatra *et al.*, [6] have studied two-dimensional stagnation-point flow over a stretching sheet. The flat deformable sheet is used in the model by Mahapatra *et al.*, [6], with the constant free stream velocity.

The study done by Kafoussias and Williams [7] proved that a working fluid's viscosity is dependent on the variation of parameter. The interactions between these two factors cause an occurrence of

\* Corresponding author.

E-mail address: [ctsuzilliana@upm.edu.my](mailto:ctsuzilliana@upm.edu.my) (Siti Suzilliana Putri Mohamed Isa)

error for the heat transfer process. The study done by Hussain *et al.*, [8] showed that in the presence of Casson fluid, viscosity existed with the flow passing through the contracting surface and influenced by a magnetic field. Then, Abbas *et al.*, [9] have examined the influence of viscosity and thermal conductivity of Carreau fluid with the magnetohydrodynamic boundary layer flow, while Zulkifli *et al.*, [10] has found viscous dissipation in a nanofluid flow, due to a moving plate.

Many researchers have considered magnetohydrodynamic (MHD) and have added various parameters for the innovations. Hayat *et al.*, [11] studied thermal radiation in MHD flow at a stretching vertical plate in a two-dimensional model. Based on the mention reviews, they used the homotopy analysis method to obtain solutions of the coupled non-linear system. Ali *et al.*, [12] have considered the steady MHD stagnation point flow with the induced magnetic field. They found that the magnetic parameter influences the variation of velocity and temperature profiles. Reddy [13] reported the case of convection in MHD Casson fluid flow. He has proposed a model which considered both assisting and opposing buoyant flows. The newest research works [14-16] have examined MHD related to viscous dissipation, Sutterby nanofluid and Carreau liquid, respectively. The study from [14] analyzed the MHD flow beyond a non-linear stretching surface with viscous dissipation. The dual solution occurred in their result. Next, Sohail and Naz [15] has done their study with the new nanofluid element (known as Sutterby) with the presence of MHD on the stretching field, while Mahanthesh [16] include Carreau liquid with MHD over a shrinking sheet.

Nanofluids are a new heat transfer fluid that contains a base fluid and nanoparticles such as copper, alumina, titania and silica from 1 to 100 nm. It has higher thermal conductivity and single-phase heat transfer coefficients than the base fluids based on Buongiorno [17]. Xuan and Li [18] have studied the thermal conductivity of nanofluids. They have proposed a theoretical model to describe the heat transfer performance of the nanofluids in a tube with the presence of solid particles. Besides that, the problem related to laminar fluid for stretching a flat surface in nanofluids is first studied by Khan and Pop [19]. This paper concluded that the Nusselt number reduced when each dimensionless number decreases, while reduced the Sherwood number increased the values of the parameters related to the research. Ahmad and Pop [20] had done their study on the mixed convection nanofluid flow past a vertical plate embedded in a porous medium. Nowadays, researchers more interested in hybrid nanofluids. The hybrid nanofluid remarks a new feature in manufacturing industrial applications. Zainal *et al.*, [21] studied hybrid nanofluid over a quadratic velocity of a stretching sheet. Meanwhile, Junoh *et al.*, [22] included a magnetic field in their research. Subsequently, Waini *et al.*, [23] studied the shrinking wedge with hybrid nanofluid.

There are many advantages of using thermal radiation, one of them is thermal radiation can cause the heat transfer rate to increase rapidly and boundary layer flow decreases [24]. Sheikholeslami *et al.*, [25] studied the problem of MHD related thermal radiation between two horizontal rotational plates. Meanwhile, Sharma *et al.*, [26] also studied thermal radiation, but they relate it with heat transfer over a permeable exponentially shrinking sheet. Sheikholeslami *et al.*, [25] used Runge-Kutta method of order four to solve the mathematical problems. Besides, Sharma *et al.*, [26] solved the ordinary differential equations using a finite difference method MATLAB software. Other than that, Adnan *et al.*, [27] studied the effect of suction, partial slip, and thermal radiation on steady MHD flow and heat transfer. Uddin *et al.*, [24] have also considered copper-water nanofluid, together with the effect of thermal radiation and exponentially permeable shrinking sheet. The dual solution introduced in the results for some values of parameters.

Slip boundary conditions play an essential role in the velocity of the fluid surfaces and coated surfaces. It is considered in some situations like perforated plates and wire nettings, as stated by Bilal [28]. MHD Newtonian fluid flow beyond a shrinking sheet subjected to the thermal slip was studied by Ahmad *et al.*, [29]. The thickness of the boundary layer has been discussed for the different types

of parameters. Moreover, considering the velocity and thermal slip, Ghosh and Mukhopadhyay [30] have investigated the exponentially porous shrinking sheet of the nanofluid flow. A dual solution was also introduced in the study for a few governing parameters. This paper concluded that the enhancement of the nanoparticle volume fraction causes the velocity and temperature of the fluid to be increased. In addition, Yang *et al.*, [31] have proposed the second-order slip model with the flow of heat transfer from a double Maxwell fluid. The results showed that the fractional Maxwell fluid gave stronger viscosity, leading to increased slip parameters. Mohamadi *et al.*, [32] have investigated slip condition at the wall with heat transfer of the internal flow nanorefrigerant. Another new study found that the pressure drop reduces using the slip boundary condition at the wall about 25%.

Therefore, this present paper extends the study from Ghosh and Mukhopadhyay [30] by adding the effect of the thermal radiation. This paper aims to investigate the impact of nanoparticle volume fraction parameter and temperature-dependent viscosity with the Nusselt number, the skin friction coefficient, velocity profile and temperature profile. The details on stability analysis have been discussed by Ghosh and Mukhopadhyay [30] in their studies.

## 2. Methodology

### 2.1 Mathematical Formulation

The study considered a steady two-dimensional boundary layer flow over an exponentially porous shrinking sheet of nanofluids with the presence of thermal radiation containing partial slip boundary conditions and suction. The water and kerosene are assumed to be base fluid. The following forms are used for the governing boundary layer equations of motion and the energy equation when Ag as nanoparticle with the Tiwari and Das [33] and Ghosh and Mukhopadhyay [30]. The mathematical model in this paper is shown as below

$$\frac{\partial u}{\partial x} + \frac{\partial v}{\partial y} = 0, \quad (1)$$

$$u \frac{\partial u}{\partial x} + v \frac{\partial u}{\partial y} = \nu_{nf} \frac{\partial^2 u}{\partial y^2}, \quad (2)$$

$$u \frac{\partial T}{\partial x} + v \frac{\partial T}{\partial y} = \frac{\kappa_{nf}}{(\rho C_p)_{nf}} \frac{\partial^2 T}{\partial y^2} - \frac{1}{(\rho C_p)_{nf}} \frac{\partial q_r}{\partial y} \quad (3)$$

where the velocity component in  $x$  and  $y$  directions are denoted by  $u$  and  $v$ , respectively,  $\nu_{nf} = \frac{\mu_{nf}}{\rho_{nf}}$  is the kinematic viscosity of the nanofluid,  $\mu_{nf}$  is the viscosity of the nanofluid,  $\rho_{nf}$  is the density of the nanofluid,  $T$  is the temperature,  $\kappa_{nf}$  is the thermal conductivity of the nanofluid, the specific heat capacity of the nanofluid is represented with  $(\rho C_p)_{nf}$ . For the radiation flux,  $q_r$  is given by Pal and Mondal [34]

$$q_r = -\frac{4\sigma^*}{3K^*} \frac{\partial T^4}{\partial y}, \quad (4)$$

where  $\sigma^*$  and  $K^*$  are the Stefan-Boltzmann constant and Rosseland absorption coefficient approximation, respectively. Next, the term  $T^4$  can be articulated as a linear function of temperature

and can be expanded by using Taylor series. Thus, the higher order terms can be ignored and it yields to

$$T^4 = 4T_\infty^3 T - 3T_\infty^4, \tag{5}$$

The fluid velocity is low with the flow being laminar and the viscous dissipative heat is expected to be negligible. Das [35] gives the effective fluid properties as follows

$$\begin{aligned} \rho_{nf} &= (1 - \phi)\rho_f + \phi\rho_s, \mu_{nf} = \frac{\mu_f}{(1-\phi)^{2.5}}, \\ (\rho C_p)_{nf} &= (1 - \phi)(\rho C_p)_f + \phi(\rho C_p)_s, \\ \frac{\kappa_{nf}}{\kappa_f} &= \frac{(2\kappa_f + \kappa_s) - 2\phi(\kappa_f - \kappa_s)}{(2\kappa_f + \kappa_s) + \phi(\kappa_f - \kappa_s)}, \end{aligned} \tag{6}$$

where  $\phi$  is denotes the solid volume fraction,  $\rho$  is the density,  $\mu$  is the dynamic viscosity and  $\kappa$  is the effective thermal conductivities. The subscripts  $nf$ ,  $s$  and  $f$  are nanofluid, nanoparticles and base fluid, respectively.

The boundary conditions are

$$u = -U_w + B' v_f \frac{\partial u}{\partial y}, v = -v_w = -v_0 e^{\frac{x}{2L}} \text{ at } y = 0 \text{ and } u \rightarrow \infty \text{ as } y \rightarrow \infty, \tag{7}$$

$$T = T_w + D' \frac{\partial T}{\partial y} \text{ at } y = 0 \text{ and } T \rightarrow T_\infty \text{ as } y \rightarrow \infty. \tag{8}$$

where  $U_w = -c e^{\frac{x}{2L}}$  is the shrinking velocity when  $c > 0$  (corresponds to the shrinking constant), and  $v_w = v_0 e^{\frac{x}{2L}}$  where  $v_0$  is the constant mass flux velocity with  $v_0 < 0$  correspond to the suction while  $v_0 > 0$  corresponds to the injection.  $T_w$  reflects the variable temperature at the sheet with  $T_0$  being a constant measuring the rate of increase in temperature along the sheet. We also have  $B' = B_1 e^{-\frac{x}{2L}}$  and  $D' = D_1 e^{-\frac{x}{2L}}$  where  $B'$  and  $D'$  are the velocity slip and thermal slip factors respectively. Thermophysical properties of the fluid phase (water), kerosene and Ag are given in Table 1 by Hussein *et al.*, [36].

**Table 1**  
 Thermophysical properties of the fluid phase (water), kerosene and Ag

	$\rho$ (kg/m <sup>3</sup> )	$C_p$ (J/kg K)	$\kappa$ (W/m K)	Pr
Water	997.1	4179	0.613	6.2
Kerosene	783	2090	0.15	21
Ag	10,500	235	429	

## 2.2 Similarity Transformations

Introduce the stream function,  $\psi$  where  $u = \partial\psi/\partial y$  and  $v = -\partial\psi/\partial x$ . Next, the following similarity transformations are considered

$$\psi = \sqrt{2\nu_f L c f(\eta)} e^{\frac{x}{2L}}, \theta(\eta) = \frac{T - T_w}{T_w - T_\infty}, \eta = y \sqrt{\frac{c}{2\nu_f L}} e^{\frac{x}{2L}} \quad (9)$$

where  $\eta$  and  $L$ , respectively, represent the similarity variable and length of characteristic. Substituting Eq. (4), (7), (8) and (9) into Eq. (2) and (3) lead to the following equations

$$\frac{1}{(1-\phi)^{2.5} \left(1 - \phi + \phi \frac{\rho_s}{\rho_f}\right)} f'''' + f'' f - 2f'^2 = 0, \quad (10)$$

$$\frac{1}{(1-\phi) + \phi \frac{(\rho C_p)_s}{(\rho C_p)_f}} \left[ \frac{\kappa_{nf}}{\kappa_f} + \frac{4}{3} Rd \right] \theta'' + Pr(f\theta' - f'\theta) = 0, \quad (11)$$

where  $Rd = \frac{4\rho T_\infty^3}{\kappa \times \kappa_f}$  is the radiation parameter and  $Pr = (\mu C_p)_f / \kappa_f$  is the Prandtl number. Note that the primes in Eq. (10) and (11) denote the differentiation with each of the function respect to  $\eta$ .

The boundary conditions are transformed and obtained

$$f(\eta) = S, f'(\eta) = -1 + Bf''(\eta) \text{ at } \eta = 0, f'(\eta) \rightarrow 0 \text{ as } \eta \rightarrow \infty, \quad (12)$$

$$\theta(\eta) = 1 + D\theta'(\eta), \text{ at } \eta = 0, \theta(\eta) \rightarrow 0 \text{ as } \eta \rightarrow \infty, \quad (13)$$

where  $S = -\frac{v_0}{\sqrt{(v_f c)/2L}}$  corresponds to the suction or blowing parameter. In our research, when

$S > 0$  and also  $v_0 < 0$  are aligns to suction while  $S < 0$  and also  $v_0 > 0$  are aligns to blowing

$B = B_1 \sqrt{\frac{c\nu_f}{2L}}$  and  $D = D_1 \sqrt{\frac{c}{2\nu_f L}}$  are the velocity slip and thermal slip parameters, respectively.

In practical applications, the physical quantities of principal interest are the skin friction coefficients,  $C_f$  and the Nusselt number,  $Nu_x$  which are defined as

$$C_f = \frac{\mu_{nf}}{\rho_f U_w^2} \left. \frac{du}{e^{\frac{x}{2L}} dy} \right|_{y=0}, \quad Nu_x = - \left. \frac{x \kappa_{nf}}{\kappa_f (T_w - T_\infty)} \frac{dT}{dy} \right|_{y=0}. \quad (14)$$

By substituting Eq. (9) and (7) into Eq. (14), the skin friction and Nusselt number can be arranged as

$$C_f Re_x^{\frac{1}{2}} = \frac{1}{(1-\phi)^{2.5}} f''(0), \quad Nu_x Re_x^{-\frac{1}{2}} = - \frac{\kappa_{nf}}{\kappa_f} \left[ 1 + \frac{4}{3} Rd \left( \frac{\kappa_{nf}}{\kappa_f} \right)^{-1} \theta'(0) \right]. \quad (15)$$

### 3. Results and Discussion

In this study, the parameter that is fixed are Prandtl number ( $Pr = 6.2$  for Ag-Water and  $Pr = 21$  for Ag-kerosene), thermal radiation  $Rd = 1.0$ , and temperature  $T = 0.1$ . The obtained results are presented graphically to show the various parameters given in Figure 1, Figure 2, and Figure 3 for

velocity and temperature profile, while Figure 4, Figure 5 and Figure 6 present the results of skin friction and Nusselt number, respectively. There are dual solutions: first branch (solid line) and second branch solution (dashed line).

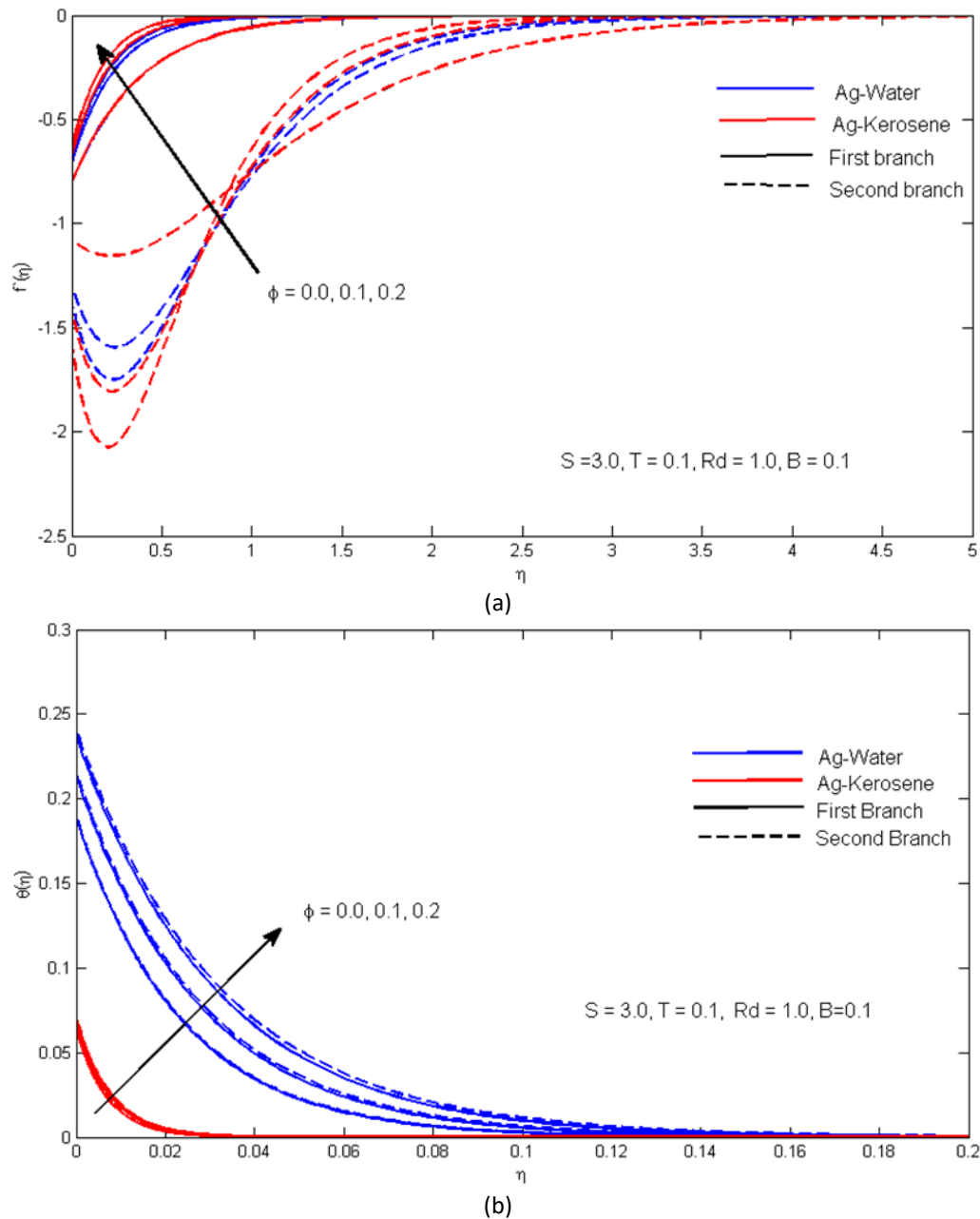


**Fig. 1.** Various values of nanoparticle volume  $\phi$  on (a) velocity profile  $f'(\eta)$  and (b) temperature profile  $\theta(\eta)$

Figure 1(a) presents the dual velocity profiles for variation of nanoparticle volume fraction,  $\phi$ . The first branch solution in Figure 1(a) shows that the fluid velocity increases due to the rise in  $\phi$ . This increment is valid for both Ag-Water and Ag-Kerosene. Then, Figure 1(a) also shows a different second branch solution than the first branch solution, but the velocity profile still has the same behaviour. Thus, the increase in the nanoparticle volume fraction will cause the fluid flow to travel rapidly. Next, Figure 1(b) displays the dual temperature profiles for the difference in  $\phi$ . According to the observation, the temperature of Ag-Water is higher than Ag-Kerosene in Figure 1(b). Therefore,

we may infer that a rise in nanofluid thermal conductivity is dependent on the increment in nanoparticle volume fraction.

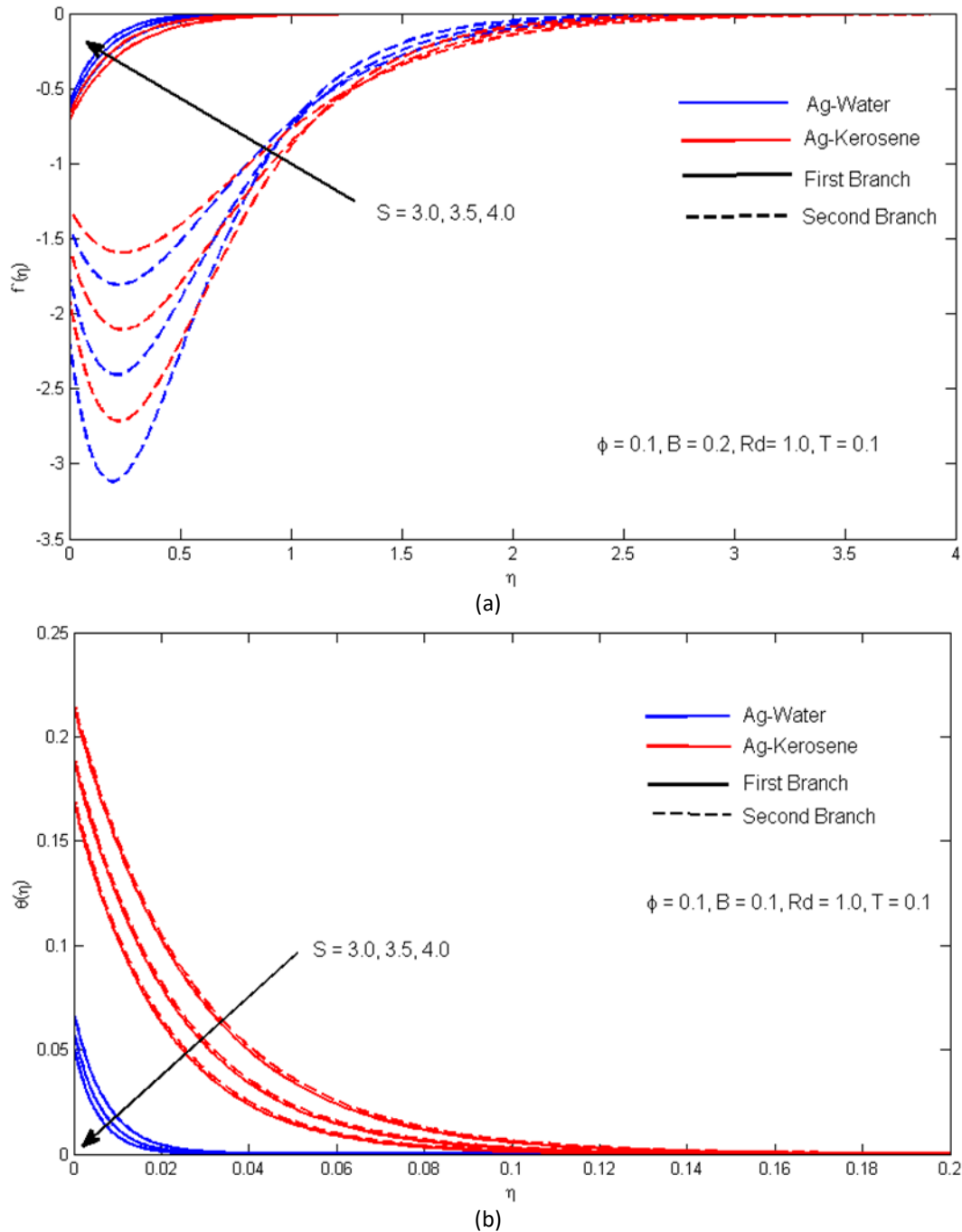


**Fig. 2.** Various values of the suction parameter  $S$  on (a) velocity profile  $f'(\eta)$  and (b) temperature profile  $\theta(\eta)$

Figures 2(a) and 2(b) displays the various values of effect on the suction parameter,  $S$  on the velocity and temperature profile. As a result, the increase of  $S$  causes the values of velocity profile to increase. This condition happens because the rate of suction increases while the thickness of the velocity boundary layer reduces, as confirmed by Ghosh and Mukhopadhyay [30]. Figure 2(b) shows a decrease in fluid temperature has been identified due to an increase of  $S$ . Thus, the thickness of

the boundary layer would become thinner. Compared to nanofluid Ag-water, it can be seen from the graph that Ag-Kerosene has a lower boundary layer thickness.

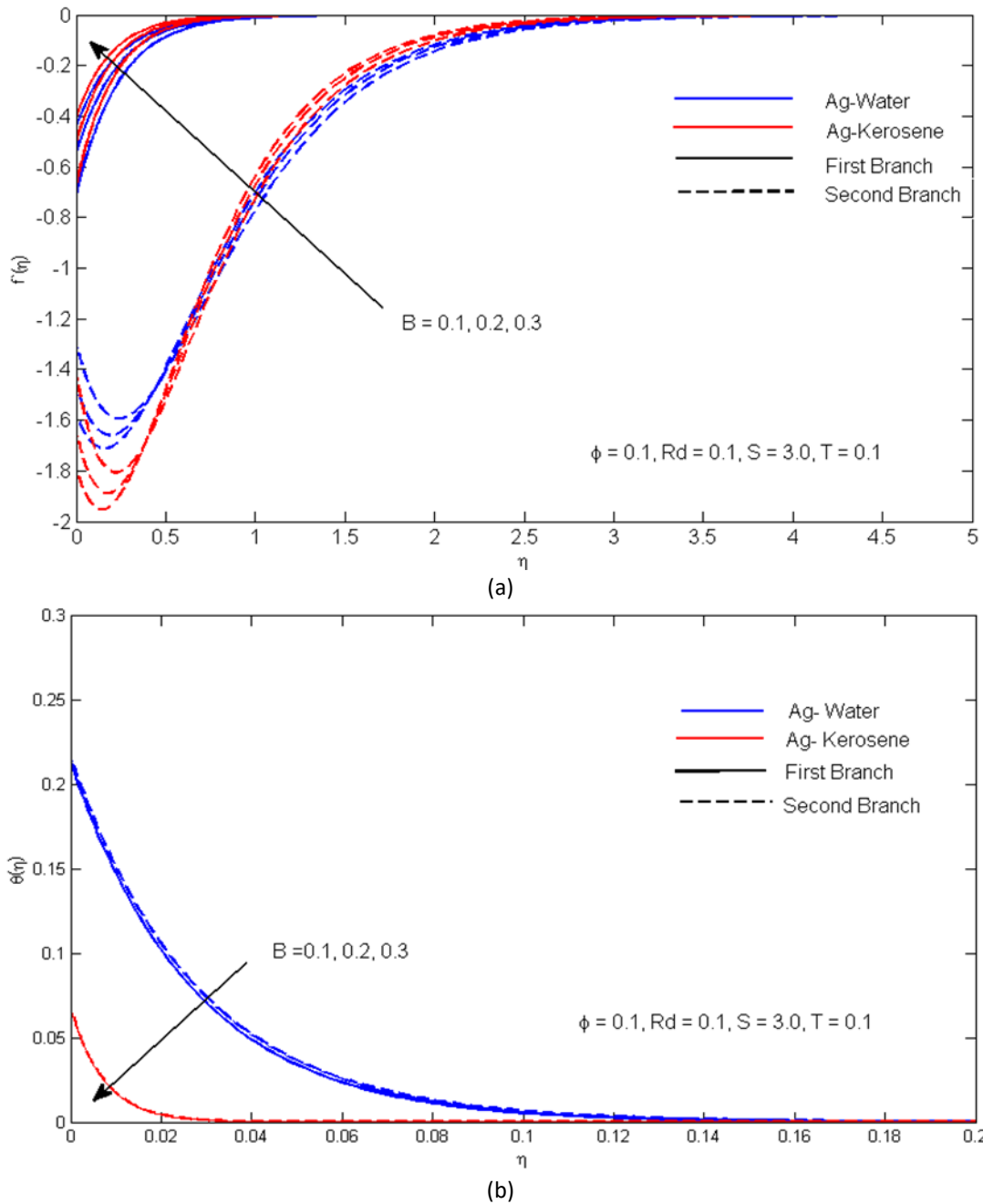


**Fig. 3.** Various values of slip parameter  $B$  on (a) velocity profile  $f'(\eta)$  and (b) temperature profile  $\theta(\eta)$

Further, the graph of velocity and temperature profile with different values of slip parameter  $B$  are shown in Figure 3(a) and (b). It is observed that velocity increases as  $B$  increases on the first branch solution while initially decreasing and increasing during the second branch solution as depicted in Figure 3(a). On the other hand, from Figure 3(b), the temperature profile decreases when  $B$  increase. This condition is due to the decrease in the thermal boundary layer thickness when reacting to  $B$ .



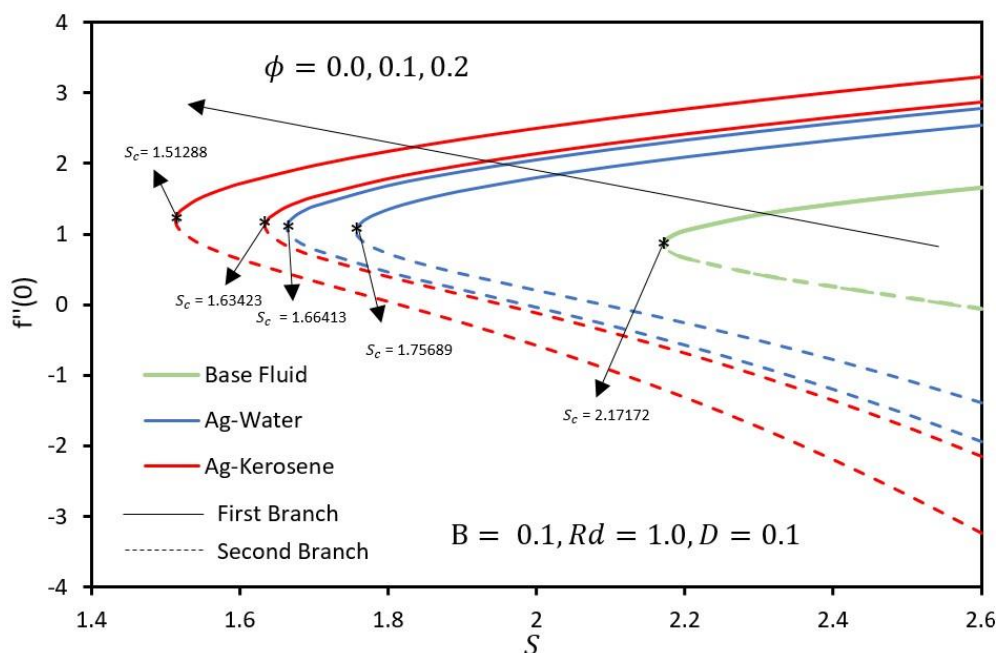
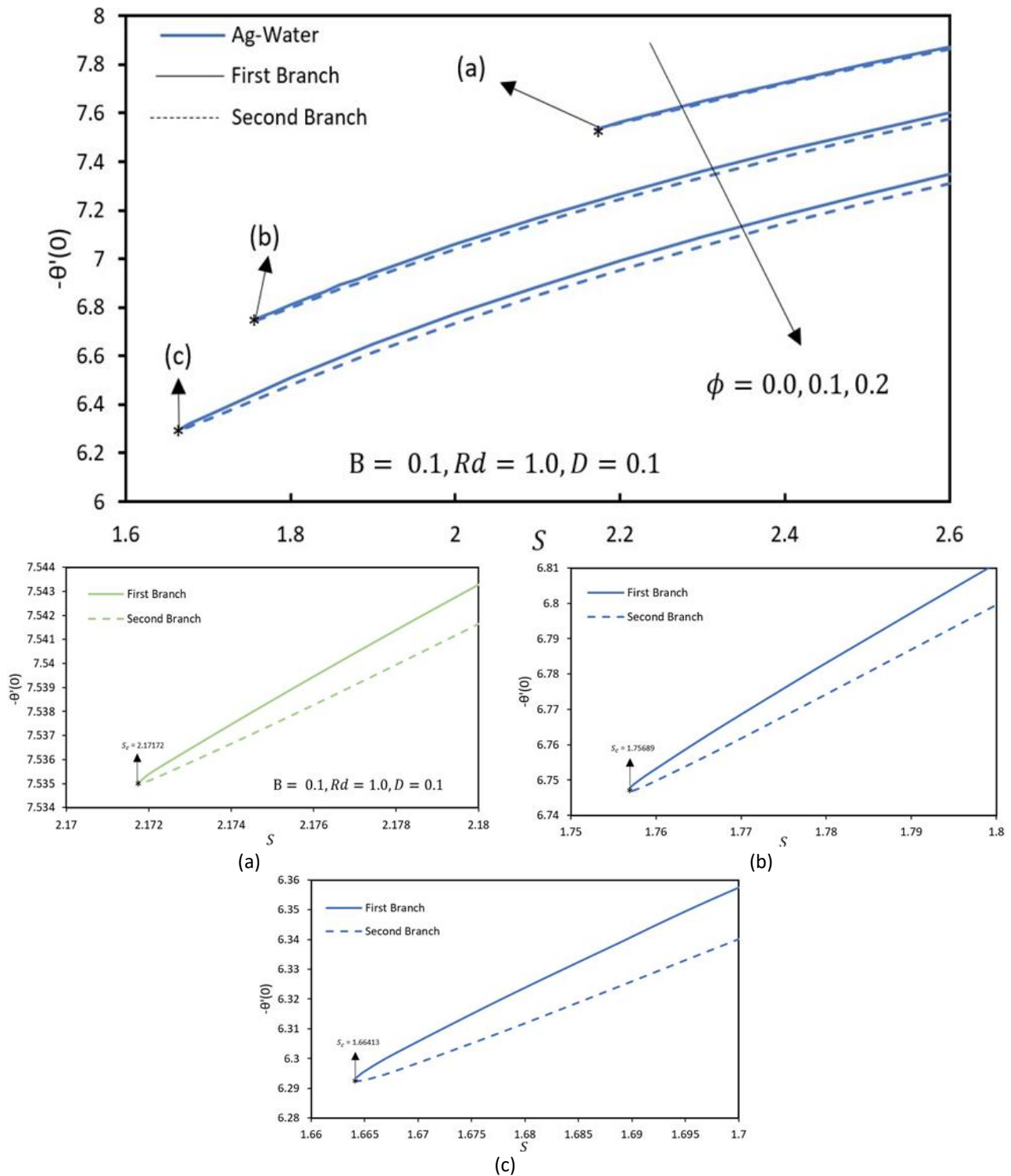


**Fig. 4.** Various values of the suction parameter  $S$  on  $f''(0)$  with different values of nanoparticle volume fraction,  $\phi$

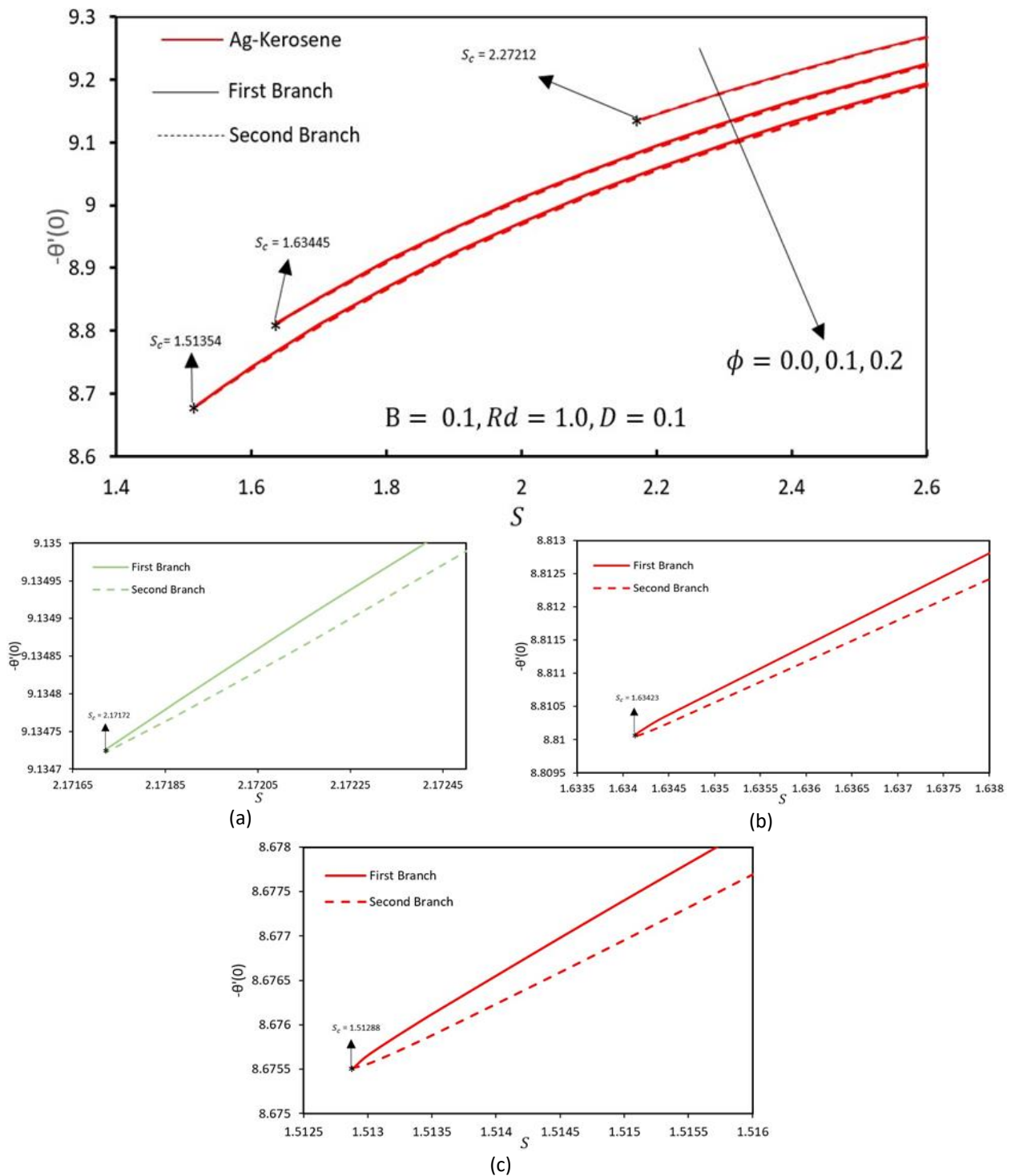
Furthermore, Figure 4, 5 and 6 show the skin friction coefficient and Nusselt number with various values of  $\phi$ . The skin friction coefficient with the different values of  $S$  on multiple values of  $\phi$  is revealed in Figure 4. The intersection point between both branches is denoted by critical suction point  $S_c$ . The local skin friction coefficient increases for the first branch solution due to the rise in  $\phi$  and  $S$ . In the second branch, the opposite effect is observed. For the base fluid,  $\phi = 0$ , the value of critical suction number is  $S_c = 2.17172$ . On the other hand, dual solutions of Ag-Water can be seen at  $S_c = 1.75689$  ( $\phi = 0.1$ ) and  $S_c = 1.66413$  ( $\phi = 0.2$ )., Moreover, the critical suction points for Ag-kerosene are  $S_c = 1.63423$  and  $S_c = 1.51288$  for both  $\phi = 0.1, 0.2$ , respectively.

Figure 5 represents the Nusselt number which has various values of  $\phi$ , only for Ag-Water. This figure shows the Nusselt number increases due to  $S$ , and decreases due to  $\phi$ . For the largest  $\phi$ , the critical suction point is recorded as the highest point. Thus, compared to the stretching surface, the value of the Nusselt number appears lower with the shrinking surface. As a result, the stretching flat plate occurred due to the low exposed area of the shrinking flat plate as approved by Naganthran *et al.*, [37].

Figure 6 illustrates the effect of the suction parameter on the Nusselt number with different values of  $\phi$  for Ag-kerosene only. Further, the values of the Nusselt number are found to increase with the suction parameter increases. In addition, with the rise in  $\phi$  leads to the decrement in the Nusselt number for both solutions. Precisely, it is due to the lack of magnitude of the suction parameter, as indicated by Jamaludin [38]. Thus, the three figures (Figure 4, 5 and 6) prove the concept by Jamaludin [38] if  $S_c < S$ .



**Fig. 5.** Various values of the suction parameter  $S$  on  $-\theta'(0)$  for Ag-Water when (a)  $S_c = 2.17172$  (b)  $S_c = 1.75689$  and (c)  $S_c = 1.66413$



**Fig. 6.** Various values of the suction parameter  $S$  on  $-\theta'(0)$  for Ag-Kerosene when (a)  $S_c = 2.1712$  (b)  $S_c = 1.63423$  and (c)  $S_c = 1.51288$

#### 4. Conclusions

Similarity transformations have been introduced to reduce partial differential equations to ordinary differential equations. Ordinary differential equations and boundary conditions were solved by using bvp4c solver. As a result, there are two different solutions (first branch solution and second branch solution) for various parameters and the velocity profile increases when both nanoparticle volume fraction,  $\phi$  and suction parameter,  $S$  increase. While the increasing in suction parameter,  $S$

leads to the decreasing in the temperature profile. Besides that, skin friction coefficient and Nusselt number increase when the suction parameter,  $S$  increases.

## Acknowledgement

This research was funded by a grant from the Ministry of Higher Education of Malaysia through FRGS/1/2020/STG06/UPM/02/1

## References

- [1] Sheikholeslami, Mohsen, Davood Domiri Ganji, M. Younus Javed, and R. Ellahi. "Effect of thermal radiation on magnetohydrodynamics nanofluid flow and heat transfer by means of two phase model." *Journal of Magnetism and Magnetic Materials* 374 (2015): 36-43. <https://doi.org/10.1016/j.jmmm.2014.08.021>
- [2] Sakiadis, B. C. "Boundary layer behaviour on continuous solid surfaces. 1." *Boundary layer equations for two-dimensional and axisymmetric flow 2* (1960): 26-28. <https://doi.org/10.1002/aic.690070108>
- [3] Rajagopal, Kumbakonam R., T. Y. Na, and A. S. Gupta. "Flow of a viscoelastic fluid over a stretching sheet." *Rheologica Acta* 23, no. 2 (1984): 213-215. <https://doi.org/10.1007/BF01332078>
- [4] Vajravelu, K. "Viscous flow over a nonlinearly stretching sheet." *Applied mathematics and computation* 124, no. 3 (2001): 281-288. [https://doi.org/10.1016/S0096-3003\(00\)00062-X](https://doi.org/10.1016/S0096-3003(00)00062-X)
- [5] Khan, W. A., and I. Pop. "Boundary-layer flow of a nanofluid past a stretching sheet." *International journal of heat and mass transfer* 53, no. 11-12 (2010): 2477-2483. <https://doi.org/10.1016/j.ijheatmasstransfer.2010.01.032>
- [6] Mahapatra, T. Ray, and A. S. Gupta. "Heat transfer in stagnation-point flow towards a stretching sheet." *Heat and Mass transfer* 38, no. 6 (2002): 517-521. <https://doi.org/10.1007/s002310100215>
- [7] Kafoussias, N. G., and E. W. Williams. "The effect of temperature-dependent viscosity on free-forced convective laminar boundary layer flow past a vertical isothermal flat plate." *Acta Mechanica* 110, no. 1 (1995): 123-137. <https://doi.org/10.1007/BF01215420>
- [8] Hussain, Azad, Sana Afzal, Rizwana Rizwana, and M. Y. Malik. "MHD stagnation point flow of a Casson fluid with variable viscosity flowing past an extending/shrinking sheet with slip effects." *Physica A: Statistical Mechanics and Its Applications* 553 (2020): 124080. <https://doi.org/10.1016/j.physa.2019.124080>
- [9] Abbas, Tariq, Sajid Rehman, Rehan Ali Shah, Muhammad Idrees, and Mubashir Qayyum. "Analysis of MHD Carreau fluid flow over a stretching permeable sheet with variable viscosity and thermal conductivity." *Physica A: Statistical Mechanics and its Applications* 551 (2020): 124225. <https://doi.org/10.1016/j.physa.2020.124225>
- [10] Zulkifli, Siti Norfatimah, Norhafizah Md Sarif, and Mohd Zuki Salleh. "Numerical solution of boundary layer flow over a moving plate in a nanofluid with viscous dissipation: A revised model." *Journal of Advanced Research in Fluid Mechanics and Thermal Sciences* 56, no. 2 (2019): 287-295.
- [11] Hayat, T., Z. Abbas, I. Pop, and S. Asghar. "Effects of radiation and magnetic field on the mixed convection stagnation-point flow over a vertical stretching sheet in a porous medium." *International Journal of Heat and Mass Transfer* 53, no. 1-3 (2010): 466-474. <https://doi.org/10.1016/j.ijheatmasstransfer.2009.09.010>
- [12] Ali, F. M., R. Nazar, N. M. Arifin, and I. Pop. "MHD stagnation-point flow and heat transfer towards stretching sheet with induced magnetic field." *Applied Mathematics and Mechanics* 32, no. 4 (2011): 409-418. <https://doi.org/10.1007/s10483-011-1426-6>
- [13] Reddy, P. Bala Anki. "Magnetohydrodynamic flow of a Casson fluid over an exponentially inclined permeable stretching surface with thermal radiation and chemical reaction." *Ain Shams Engineering Journal* 7, no. 2 (2016): 593-602. <https://doi.org/10.1016/j.asej.2015.12.010>
- [14] Lund, Liaquat Ali, Zurni Omar, Jawad Raza, and Ilyas Khan. "Magnetohydrodynamic flow of Cu-Fe 3 O 4/H 2 O hybrid nanofluid with effect of viscous dissipation: Dual similarity solutions." *Journal of Thermal Analysis and Calorimetry* (2020): 1-13. <https://doi.org/10.1007/s10973-020-09602-1>
- [15] Sohail, Muhammad, and Rahila Naz. "Modified heat and mass transmission models in the magnetohydrodynamic flow of Sutterby nanofluid in stretching cylinder." *Physica A: Statistical Mechanics and its Applications* 549 (2020): 124088. <https://doi.org/10.1016/j.physa.2019.124088>
- [16] Mahanthesh, B. "Magnetohydrodynamic flow of Carreau liquid over a stretchable sheet with a variable thickness." *Multidiscipline Modeling in Materials and Structures* (2020). <https://doi.org/10.1108/MMMS-11-2019-0205>
- [17] Buongiorno, Jacopo. "Convective transport in nanofluids." (2006): 240-250. <https://doi.org/10.1115/1.2150834>
- [18] Xuan, Yimin, and Qiang Li. "Heat transfer enhancement of nanofluids." *International Journal of heat and fluid flow* 21, no. 1 (2000): 58-64. [https://doi.org/10.1016/S0142-727X\(99\)00067-3](https://doi.org/10.1016/S0142-727X(99)00067-3)
- [19] Khan, W. A., and I. Pop. "Boundary-layer flow of a nanofluid past a stretching sheet." *International journal of heat and mass transfer* 53, no. 11-12 (2010): 2477-2483. <https://doi.org/10.1016/j.ijheatmasstransfer.2010.01.032>

- [20] Ahmad, Syakila, and Ioan Pop. "Mixed convection boundary layer flow from a vertical flat plate embedded in a porous medium filled with nanofluids." *International Communications in Heat and Mass Transfer* 37, no. 8 (2010): 987-991. <https://doi.org/10.1016/j.icheatmasstransfer.2010.06.004>
- [21] Zainal, Nurul Amira, Roslinda Nazar, Kohilavani Naganthran, and Ioan Pop. "Stability analysis of MHD hybrid nanofluid flow over a stretching/shrinking sheet with quadratic velocity." *Alexandria Engineering Journal* 60, no. 1 (2021): 915-926. <https://doi.org/10.1016/j.aej.2020.10.020>
- [22] Junoh, Mohamad Mustaqim, Fadzilah Md Ali, Norihan Md Arifin, Norfifah Bachok, and Ioan Pop. "MHD stagnation-point flow and heat transfer past a stretching/shrinking sheet in a hybrid nanofluid with induced magnetic field." *International Journal of Numerical Methods for Heat & Fluid Flow* (2019). <https://doi.org/10.1108/HFF-06-2019-0500>
- [23] Waini, I., A. Ishak, and I. Pop. "MHD flow and heat transfer of a hybrid nanofluid past a permeable stretching/shrinking wedge." *Applied Mathematics and Mechanics* 41, no. 3 (2020): 507-520. <https://doi.org/10.1007/s10483-020-2584-7>
- [24] Uddin, M. S., A. Zaib, and K. Bhattacharyya. "Effect of thermal radiation on heat transfer in an unsteady copper-water nanofluid flow over an exponentially shrinking porous sheet." *Journal of Applied Mechanics and Technical Physics* 58, no. 4 (2017): 670-678. <https://doi.org/10.1134/S0021894417040113>
- [25] Sheikholeslami, M., T. Hayat, and A. Alsaedi. "MHD free convection of Al<sub>2</sub>O<sub>3</sub>-water nanofluid considering thermal radiation: a numerical study." *International Journal of Heat and Mass Transfer* 96 (2016): 513-524. <https://doi.org/10.1016/j.ijheatmasstransfer.2016.01.059>
- [26] Sharma, Rajesh, Anuar Ishak, Roslinda Nazar, and Ioan Pop. "Boundary layer flow and heat transfer over a permeable exponentially shrinking sheet in the presence of thermal radiation and partial slip." *Journal of Applied Fluid Mechanics* 7, no. 1 (2014): 125-134. <https://doi.org/10.36884/jafm.7.01.19489>
- [27] Adnan, Nurul Shahirah Mohd, Norihan Md Arifin, Norfifah Bachok, and Fadzilah Md Ali. "Stability analysis of MHD flow and heat transfer passing a permeable exponentially shrinking sheet with partial slip and thermal radiation." *CFD Letters* 11, no. 12 (2019): 34-42.
- [28] Ahmad, Saeed, Muhammad Yousaf, Amir Khan, and Gul Zaman. "Magnetohydrodynamic fluid flow and heat transfer over a shrinking sheet under the influence of thermal slip." *Heliyon* 4, no. 10 (2018): e00828. <https://doi.org/10.1016/j.heliyon.2018.e00828>
- [29] Bilal, M. "Micropolar flow of EMHD nanofluid with non-linear thermal radiation and slip effects." *Alexandria Engineering Journal* 59, no. 2 (2020): 965-976. <https://doi.org/10.1016/j.aej.2020.03.023>
- [30] Ghosh, Sudipta, and Swati Mukhopadhyay. "Stability analysis for model-based study of nanofluid flow over an exponentially shrinking permeable sheet in presence of slip." *Neural Computing and Applications* (2019): 1-11. <https://doi.org/10.1007/s00521-019-04221-w>
- [31] Yang, Weidong, Xuehui Chen, Zeyi Jiang, Xinru Zhang, and Liancun Zheng. "Effect of slip boundary condition on flow and heat transfer of a double fractional Maxwell fluid." *Chinese Journal of Physics* 68 (2020): 214-223. <https://doi.org/10.1016/j.cjph.2020.09.003>
- [32] Mohamadi, S., M. H. Yazdi, E. Solomin, A. Fudholi, K. Sopian, and Perk Lin Chong. "Heat transfer and entropy generation analysis of internal flow of nanorefrigerant with slip condition at wall." *Thermal Science and Engineering Progress* 22 (2021): 100829. <https://doi.org/10.1016/j.tsep.2020.100829>
- [33] Tiwari, Raj Kamal, and Manab Kumar Das. "Heat transfer augmentation in a two-sided lid-driven differentially heated square cavity utilizing nanofluids." *International Journal of heat and Mass transfer* 50, no. 9-10 (2007): 2002-2018. <https://doi.org/10.1016/j.ijheatmasstransfer.2006.09.034>
- [34] Pal, Dulal, and Hiranmoy Mondal. "Influence of temperature-dependent viscosity and thermal radiation on MHD forced convection over a non-isothermal wedge." *Applied Mathematics and Computation* 212, no. 1 (2009): 194-208. <https://doi.org/10.1016/j.amc.2009.02.013>
- [35] Das, Kalidas. "Cu-water nanofluid flow and heat transfer over a shrinking sheet." *Journal of Mechanical Science and Technology* 28, no. 12 (2014): 5089-5094. <https://doi.org/10.1007/s12206-014-1130-2>
- [36] Hussain, S. T., Sohail Nadeem, and Rizwan Ul Haq. "Model-based analysis of micropolar nanofluid flow over a stretching surface." *The European Physical Journal Plus* 129, no. 8 (2014): 1-10. <https://doi.org/10.1140/epjp/i2014-14161-8>
- [37] Naganthran, Kohilavani, Roslinda Nazar, and Ioan Pop. "Stability analysis of impinging oblique stagnation-point flow over a permeable shrinking surface in a viscoelastic fluid." *International Journal of Mechanical Sciences* 131 (2017): 663-671. <https://doi.org/10.1016/j.ijmecsci.2017.07.029>
- [38] Jamaludin, Anuar, Roslinda Nazar, and Ioan Pop. "Mixed convection stagnation-point flow of a nanofluid past a permeable stretching/shrinking sheet in the presence of thermal radiation and heat source/sink." *Energies* 12, no. 5 (2019): 788. <https://doi.org/10.3390/en12050788>